Published in "Brain Research 1536: 107–118, 2013"
which should be cited to refer to this work.

Visual thalamocortical circuits in parvalbumin-deficient mice

Alessandra Lintas[a,b], *Beat Schwaller*[a], *Alessandro E.P. Villa*[b,c,*]

[a]*Department of Medicine/ Anatomy, University of Fribourg, Switzerland*
[b]*Neuroheuristic Research Group, Information Science Institute, University of Lausanne, Switzerland*
[c]*INSERM U836; Grenoble Institute of Neuroscience; Université Joseph Fourier, Eq7 Nanomédecine et Cerveau, Grenoble, France*

The dorsal lateral geniculate nucleus (dLGN) is considered as the visual gateway to the visual cortex (VC) and sends collaterals to the thalamic reticular nucleus (RTN) that in turn receives collaterals of the corticofugal feedback projections. At all levels of this thalamocortical circuit there are GABAergic neurons expressing the calcium-buffer parvalbumin (PV). The present study reports for the first time the analysis of in vivo extracellular electrophysiological recordings performed simultaneously in dLGN, RTN and VC of anesthetized wild-type (WT) and parvalbumin-deficient (PVKO) mice. The firing rates of VC and RTN cells were increased in PVKO during spontaneous activity as well as in the presence of a photic stimulation (strobe flash at 2.5 Hz). Interestingly, dLGN cells in PVKO did not show significant changes in the rate of firing in comparison to WT. dLGN responses to the light flashes were characterized by ripples of inhibition and phasic excitation/rebound. We have analyzed the pattern of functional interactions between pairs of neighboring cells in VC, dLGN and RTN and across these areas in simultaneously recorded thalamocortical triplets, with one neuron from each area. We found that in PVKO the strength of the interactions tended to decrease locally, between neighboring cells, but tended to increase across the areas. The combination of these analyses provides new evidence on the important role played by PV-expression in regulating information processing in the central visual pathway suggesting that the ability to process information along parallel channels is decreased in the thalamocortical pathway of PV-deficient mice.

1. Introduction

Parvalbumin (PV) is a Ca^{2+}-binding protein that can act as an endogenous Ca^{2+} buffer and is localized in fast-contracting muscles, where its levels are highest, and in the brain and some endocrine tissues (Schwaller, 2010, 2012a). PV is characterized by a slow-onset Ca^{2+} binding that generally does not affect the initial amplitude of Ca^{2+} transients, but then accelerates the decay phase, thus often converting a monoexponential $[Ca^{2+}]_i$ decay into a bi-exponential one

*Corresponding author at: Neuroheuristic Research Group, University of Lausanne, Switzerland.
Fax: +41 21 692 3585.
E-mail address: avilla@nhrg.org (A.E.P. Villa).

(Collin et al., 2005; Lee et al., 2000). The acceleration of the early phase of $[Ca^{2+}]_i$ decay associated to PV activity limits or slows down the buildup of residual $[Ca^{2+}]_i$ in presynaptic terminals, thus affecting short-term plasticity (Caillard et al., 2000; Vreugdenhil et al., 2003). Several observations indicate that a decrease in the expression of PV is likely to lead to behavioral and neurochemical alterations that have been associated to epileptic seizure susceptibility (Marco et al., 1997; Schwaller et al., 2004; Farré-Castany et al., 2007), schizophrenia (Pinault, 2011; Lewis et al., 2012) and autism spectrum disorder (Oblak et al., 2011). The hypothesis is that elimination of PV produces alterations of brain development during specific periods of pre or postnatal life (Heizmann and Braun, 1992). Nowadays PV knockout (PVKO) mice represent an essential animal model to study the effects of absence of PV (Schwaller, 2012b).

Parvalbumin is highly expressed in GABAergic neurons (Celio, 1990) and the reactivity for the perineuronal net marker around GABAergic neurons confirmed that GABAergic neurons are still viable in PVKO mice (Schwaller et al., 2004). Specific parvalbumin immunoreactivity (PV-ir) was identified within subpopulations of ganglion and amacrine cells of the mouse retina (Endo et al., 1986; Sanna et al., 1993; Kim and Jeon, 2006). However, the study of the functional properties of the visual pathway of mice has attracted limited attention by the neurophysiologists in the past probably because of the poor visual acuity of this species (Prusky et al., 2000). In mice, less than 3% of the entire retinofugal pathway projects ipsilaterally (Dräger and Olsen, 1980), and the number of retinal ganglion cells viewing a point in binocular space is 9 times smaller for the ipsilateral than for the contralateral retina (Dräger and Olsen, 1980). Despite such disparity in retinofugal projections the contralateral-to-ipsilateral ratio of visually evoked responses is only 2 times smaller for the ipsilateral than for the contralateral retina at the level of the primary visual cortex (Coleman et al., 2009).

Inputs from the retina are sent from the ascending retinal ganglion cells via the optic tract to the dorsal lateral geniculate nucleus (dLGN), which serves as the obligatory pathway for visual information transfer from the retina to neocortex. Mouse dLGN has recently emerged as a model system in the study of thalamic circuit development (Linden et al., 2009; Bickford et al., 2010). The vast majority, approximately 80%, of the neurons of dLGN are thalamocortical (TC) neurons, also referred to as relay neurons, as they relay information from the retina to the cortex. Although clear morphological differences were reported among relay cells, TC cells are not PV-ir and an analysis of their electrophysiological properties did not reveal any additional distinguishing characteristics (Krahe et al., 2011). The remaining neurons of mouse dLGN are PV-ir GABAergic interneurons, whose density may be as low as 10–20% (Arcelli et al., 1997; Jaubert-Miazza et al., 2005) as recently confirmed by the analysis of the ultrastructure of synaptic profiles (Bickford et al., 2010). Excitatory projections from dLGN to the visual cortex send collaterals to the visual sector of the reticular thalamic nucleus (RTN) (Rafols and Valverde, 1973; Baldauf, 2010). In return the RTN, which is rich in PV-ir neurons (Jones and Hendry, 1989; Tanahira et al., 2009), sends GABA-mediated inhibitory projections back to the thalamus. The visual cortex sends glutamatergic excitatory projections back to dLGN with collaterals to RTN (Alexander et al., 2006; Petrof et al., 2012; Jurgens et al., 2012). A comprehensive, morphological study of the adult mouse visual cortex shows that PV-ir cells account for approximately 40% of GABAergic cortical interneurons (Gonchar et al., 2008). The two main types of cortical PV-ir interneurons are axon initial segment-targeting chandelier cells and soma-targeting large basket cells (del Río et al., 1994).

The geniculate relay cells can alter the retinocortical transfer of information changing their firing pattern between two modes, tonic and burst, with burst firing postulated to serve as a 'wakeup call' for the cortex (Sherman and Guillery, 2011). This firing mode is controlled by a T-type calcium channel that produces a voltage- and time-dependent I_T current (Zhan et al., 2000; Parajuli et al., 2010). The burst firing mode occurs during visual stimulation more often than in spontaneous activity in the mouse dLGN under halothane and nitrous oxide anesthesia (Grubb and Thompson, 2005). In behaving mice, dLGN bursting occurs more frequently during the inactive state, when cortex is in fact less responsive to the visual stimuli (Niell and Stryker, 2010). These findings show the complexity of the inhibitory mechanisms involving distinct roles of local dLGN interneurons and RTN GABAergic cells, thus suggesting that PV's role in dLGN is more complicated than simple calcium buffering (Augustinaite et al., 2011). In the visual cortex, inhibition appears to have a critical role in influencing the receptive field properties and the response gain of the neurons (Dräger, 1975; Hübener, 2003; Métin et al., 1988; Liu et al., 2010; Smith and Häusser, 2010). Different studies show the importance of PV in the mouse visual cortex for cortical information processing (Cardin et al., 2009; Chattopadhyaya et al., 2007) and how corticothalamic processing is regulating the activity in dLGN and RTN (Augustinaite et al., 2011; Jurgens et al., 2012).

The aim of the present work is to study the changes in activity of in vivo visual thalamocortical circuits produced by the deficiency of PV. We investigate the firing properties of dLGN, RTN and visual cortex neurons in anesthetized wildtype (WT) and PVKO mice by means of simultaneous extracellular recordings during spontaneous activity and photic stimulation by stroboscopic flashes. We report here for the first time electrophysiological results simultaneously recorded in dLGN, RTN and visual cortex neurons. However, the small size of the mouse brain makes such in vivo cellular recordings very difficult to perform and we collected only limited amount of data. Thanks to the combined study of the firing pattern, local functional interaction and functional interactions across the thalamocortical circuit, we provide new evidence on the important role played by PV-expression in regulating information processing in the central visual pathway.

2. Materials and methods

2.1. Mice

PV-deficient (PVKO) mice were originally generated on a mixed C57Bl/6J × 129/OlaHsd genetic background (Schwaller et al., 1999) and backcrossed to C57Bl/6J for 10 generations

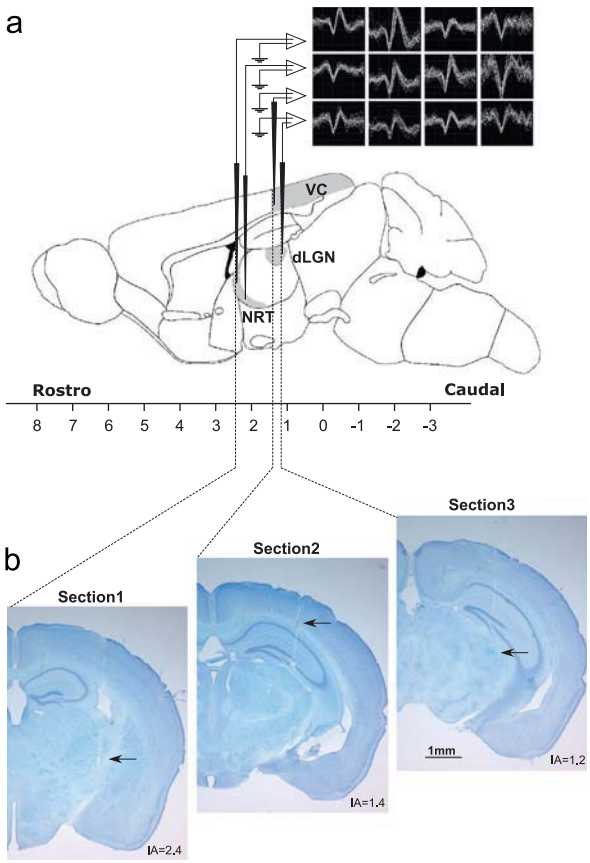

Fig. 1 – Scheme of the experimental paradigm used in this study. (A) Sagittal drawing of a mouse brain showing the three regions of interest and the oscilloscope traces of 12 single units recorded simultaneously. VC: visual cortex; dLGN: dorsal lateral geniculate nucleus; RTN: thalamic reticular nucleus. (B) Three coronal sections of mouse brain #TY1 (PVKO), stained with cresyl violet. Scale bar: 1 mm. Section 1 shows an electrode penetration in the RTN and corresponds to the rostro-caudal (interaural) coordinate IA=2.4; Section 4 shows an electrode penetration in the rostral part of VC at section IA=1.4; Section 2 shows an electrode penetration in the dLGN at section IA=1.2.

and are thus considered to be congenic to C57Bl/6J (Moreno et al., 2011); C57Bl/6J mice thus served as the control wildtype (WT) mice. All animals, including WT ones, were genotyped by PCR. Mice used for the experiments were between 3 and 5

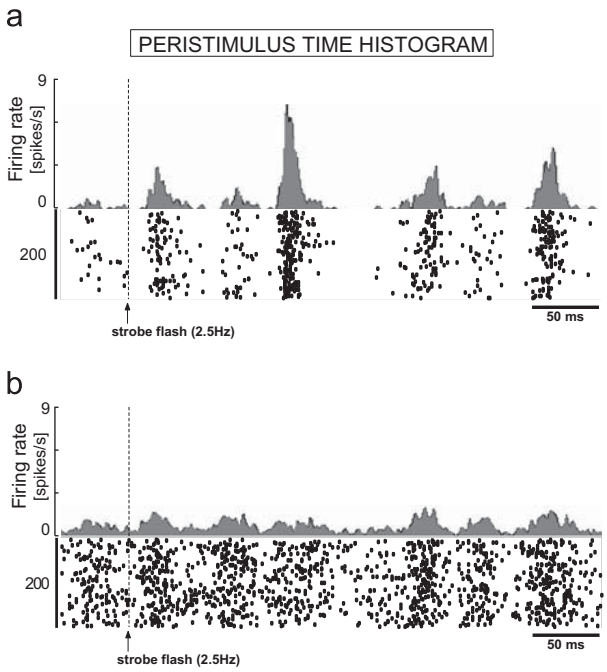

Fig. 2 – Raster plot and prestimulus time histogram (PSTH) of two cells recorded simultaneously from the same electrode tip in the dLGN of a WT mice (#TW1) during photic stimulation with strobe flash at a frequency of 2.5 Hz. (a) Notice the characteristic late peak of the excitatory response at a latency in the range 70–120 ms followed by a strong inhibitory response and ripples of activity. (b) The main pattern of response is a series of ripples attuned with the other cell's activation. Abscissa is scaled to 350 ms for all plots. Scale bar: 50 ms. The histograms are smoothed by Gaussian shaped bin of 5 ms calculated according to Abeles (1982a). The vertical dashed lines correspond to the onset of the strobe flash.

Table 1 – Firing rates (mean±S.E.M.) of the single units recorded in the visual cortex (VC), thalamic reticular nucleus (RTN) and dorsal lateral geniculate nucleus (dLGN) of wild-type (WT) and parvalbumin-deficient (PVKO) mice, during spontaneous activity and photic stimulation by strobe flash at 2.5 Hz.

Recorded area	N	Spontaneous activity	Photic stimulation
		Firing rate (spikes/s)	
VC			
WT	12	2.5±0.2	2.4±0.2
PVKO	16	5.3±0.9	6.0±0.9
RTN			
WT	26	2.0±0.6	2.1±0.6
PVKO	34	4.6±1.3	3.9±1.4
dLGN			
WT	14	3.8±1.4	6.7±2.5
PVKO	21	3.7±0.5	5.1±1.1

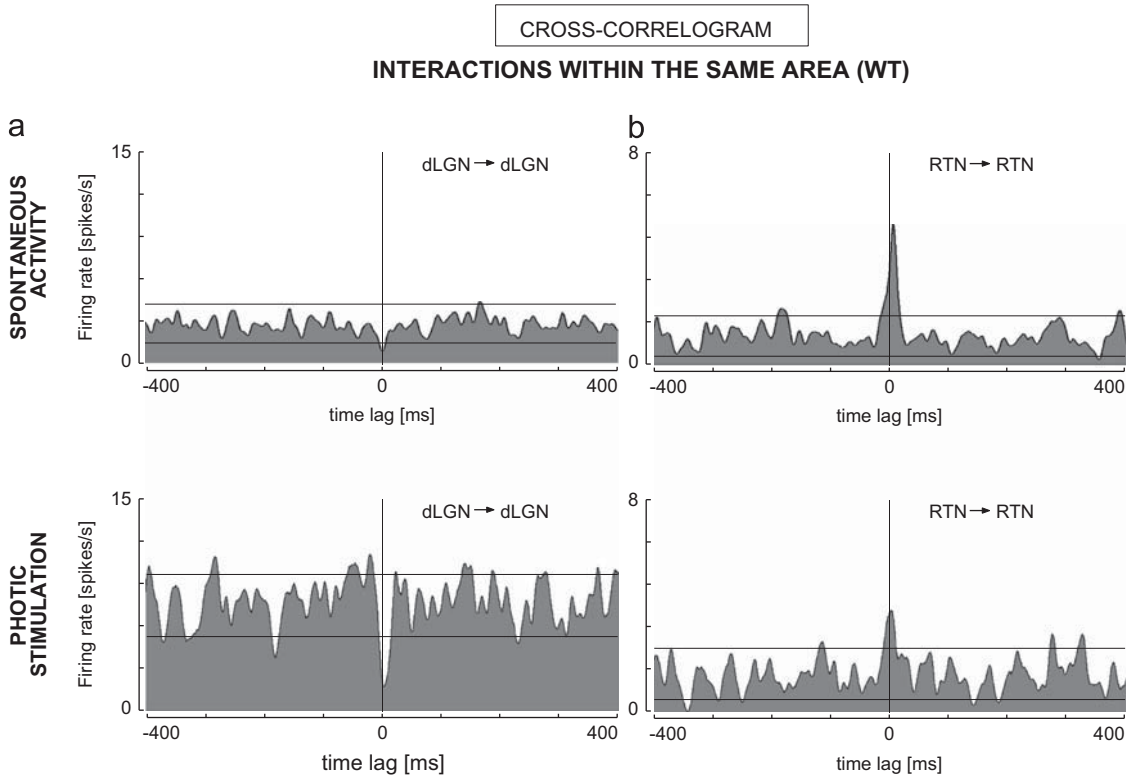

Fig. 3 – Cross-correlograms of selected pairs of neighboring units in wild-type mice. (a) Cell pair in the dorsal lateral geniculate nucleus (dLGN) (#TW1). (b) Cell pair in the thalamic reticular nucleus (RTN) (#TB1). The upper panels show the functional interactions during spontaneous activity and the lower panels during photic stimulation. The lag (ms) on the abscissa is scaled to 400 ms for all plots. The ordinate is scaled as instantaneous firing rate (spikes/s). The histograms are smoothed by a Gaussian shaped bin of 5 ms calculated according to Abeles (1982b). The two solid black horizontal lines on each panel correspond to upper and lower 99% confidence limits against a random (Poisson) distribution.

months old and weighing 25–30 g. We aimed to minimize the number of mice and all experiments were performed with the permission of the local animal care committee (Canton of Fribourg, Switzerland) and according to the present Swiss law and the European Communities Council Directive of 24 November 1986 (86/609/EEC). Animals were housed in groups of 3–5 individuals and kept under controlled conditions of light, temperature and humidity, with food and water available ad libitum.

Table 2 – Distribution of the classes of interactions between *N* neighboring cells in the visual cortex (VC), thalamic reticular nucleus (RTN) and dorsal lateral geniculate nucleus (dLGN) for wild-type (WT) and parvalbumin-deficient (PVKO) mice during spontaneous activity. *CI*: common input; *NOI*: no interaction; *other*: functional interactions other than CI.

Genotype	VC	RTN	dLGN
WT			
N	12	38	18
CI	42%	26%	33%
Other	8%	8%	6%
NOI	50%	66%	61%
PVKO			
N	18	46	30
CI	33%	20%	17%
Other	6%	9%	3%
NOI	61%	71%	80%

2.2. *Surgery and electrophysiological recordings*

The mice ($n=3$ WT and $n=4$ PVKO) were deeply anesthetized with an intraperitoneal injection of Equithesin (3 ml/kg, *i.p.*) (chloral hydrate 4.24 mg, sodium pentobarbital 0.97 mg, and magnesium sulfate $MgSO_4$ 2.13 mg in 100 ml solution with 11% ethanol, 42% propylene glycole v/v) at a dose corresponding to 130 mg/kg chloral hydrate and 30 mg/kg pentobarbital (Lintas et al., 2012). During the anesthesia the body temperature was monitored and maintained in the range 38–39 °C by means of a heating pad. The withdrawal reflex was regularly checked and heart rate monitored to detect any change in the depth of anesthesia such that supplementary doses of Equithesin were provided during the whole recording session, if necessary. The animals were mounted in a stereotaxic apparatus. All surgical wounds were infiltrated with Scandicaine 0.5% (AstraZeneca) for local anesthesia. After local opening of the skull the electrodes were driven to the surface of the brain using an electrode positioning system for independent multi-electrode placement (Villa et al., 1999). Extracellular single unit recordings were performed with four glass-coated platinum-plated tungsten microelectrodes having an impedance in the range 0.5–2 MΩ measured at a frequency of 1 kHz (Frederick Haer & Co,

Bowdoinham, Maine, USA). According to the atlas of Paxinos and Franklin (2001) we aimed one electrode in the visual cortex (VC) (IA = −0.5 to 1.6 mm interaural, ML = 1.0–3.0 mm from the midline, DV = 0.5–1.2 mm from the dura), one electrode in dLGN (IA = 0.8–1.9, ML = 2.0–2.4, DV = 2.2–2.8) and two electrodes in RTN (IA = 1.6–2.7, ML = 1.2–2.3, DV = 2.8–4.8). See Fig. 1A for a schematic illustration of the multiple electrodes experiment. Signals from the microelectrodes were amplified, filtered (400 Hz–20 kHz), viewed on an oscilloscope, and digitally recorded in WAV format (44 100 Hz sampling rate, 16 bit resolution) for computerized offline analysis. Spike sorting of the electrode signal files, based on a template matching algorithm, was able to separate up to three spikes recorded from the same channel (Aksenova et al., 2003; Asai et al., 2005). The time of spike discharges were digitally stored at a time resolution of 1 ms for later processing. The first recording session started approximately 90 min after the end of the surgical preparation. Simultaneous extracellular single-unit activity was recorded during *spontaneous activity* for at least 400 s and *visual stimulation* by xenon strobe flash at 2.5 Hz for at least 400 s. All recordings started at least 15 min after any supplementary dose of anesthetic and terminated at least 20 min before a new injection, thus assuming the recording conditions corresponded to a steady level of anesthesia.

2.3. *Histological examinations*

At the end of the experimental session (lasting in total 4–5 h) electrolytic lesions were placed at specific depths of the electrode track using 10 current pulses of 8 μA for 7 s at regular intervals of 10 s. Subjects received an overdose of sodium pentobarbital and perfused transcardially with 50 ml 0.9% NaCl immediately followed by 250 ml of fixative solution (4% paraformaldehyde in phosphate buffer 0.1 M, pH 7.3). The brains were removed and postfixed in 4% paraformaldehyde and cut into 40 μm sections using a vibratome (Leica, Germany). Sections including the visual cortex, dLGN and RTN from all animals were stained with cresyl violet for the reconstruction of the electrode tracks and localization of the electrode tracks.

2.4. *Statistical analysis*

Spike trains were analyzed by time series renewal density histograms (Abeles, 1982b). Using this technique, all histograms were scaled in rate units (spikes/s) and smoothed after convolution with a moving Gaussian-shaped bin of 5 ms width. For each histogram, the 99% confidence limits were calculated, assuming that spike occurrences followed a Poisson distribution. A one-tailed Fisher's exact *t*-test was used to compare the proportion of significant cross-correlations in both groups of rats.

3. Results

3.1. *Firing pattern*

Extracellular single units were recorded in 7 mice anesthetized with Equithesin (4 PVKO and 3 WT). The data presented here concern only those recording sites with at least one electrode in each region of interest simultaneously after histological check. Fig. 1B illustrates examples of electrolytic

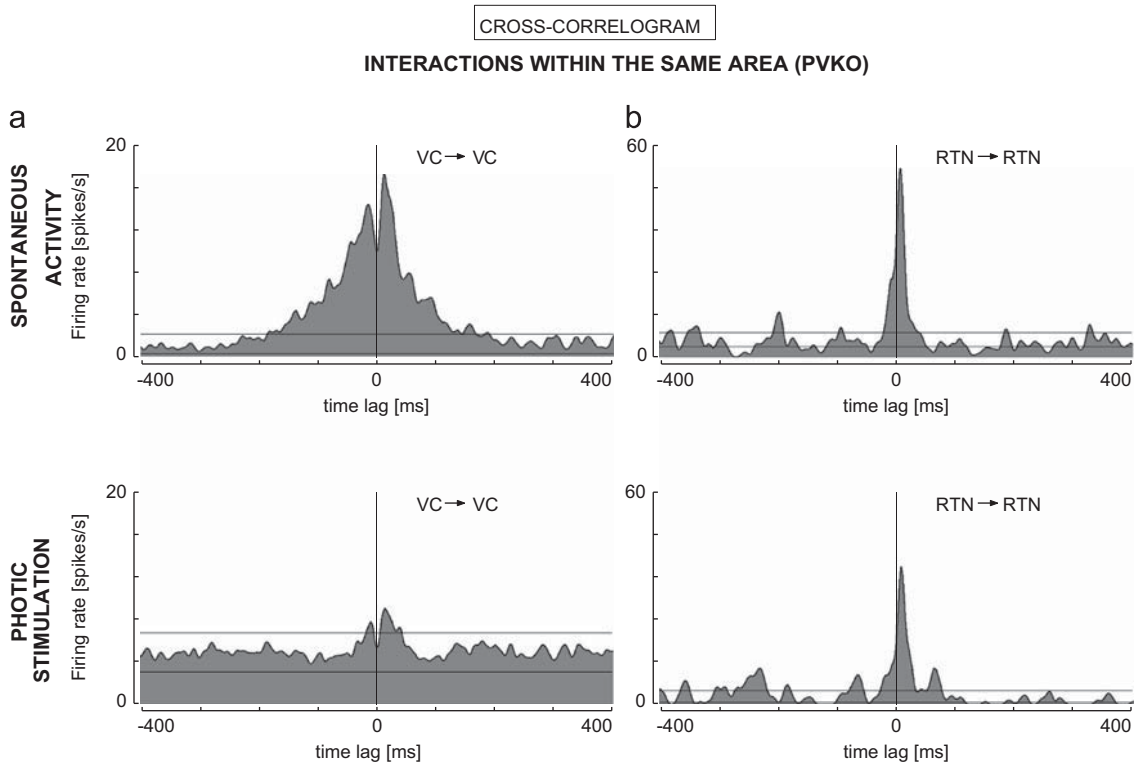

Fig. 4 – Cross-correlograms of selected pairs of neighboring units in PV-deficient mice. (a) Cell pair in the visual cortex (VC) (#TM1). (b) Cell pair in the thalamic reticular nucleus (RTN) (#TR1). For axis scaling and labels, refer to Fig. 3.

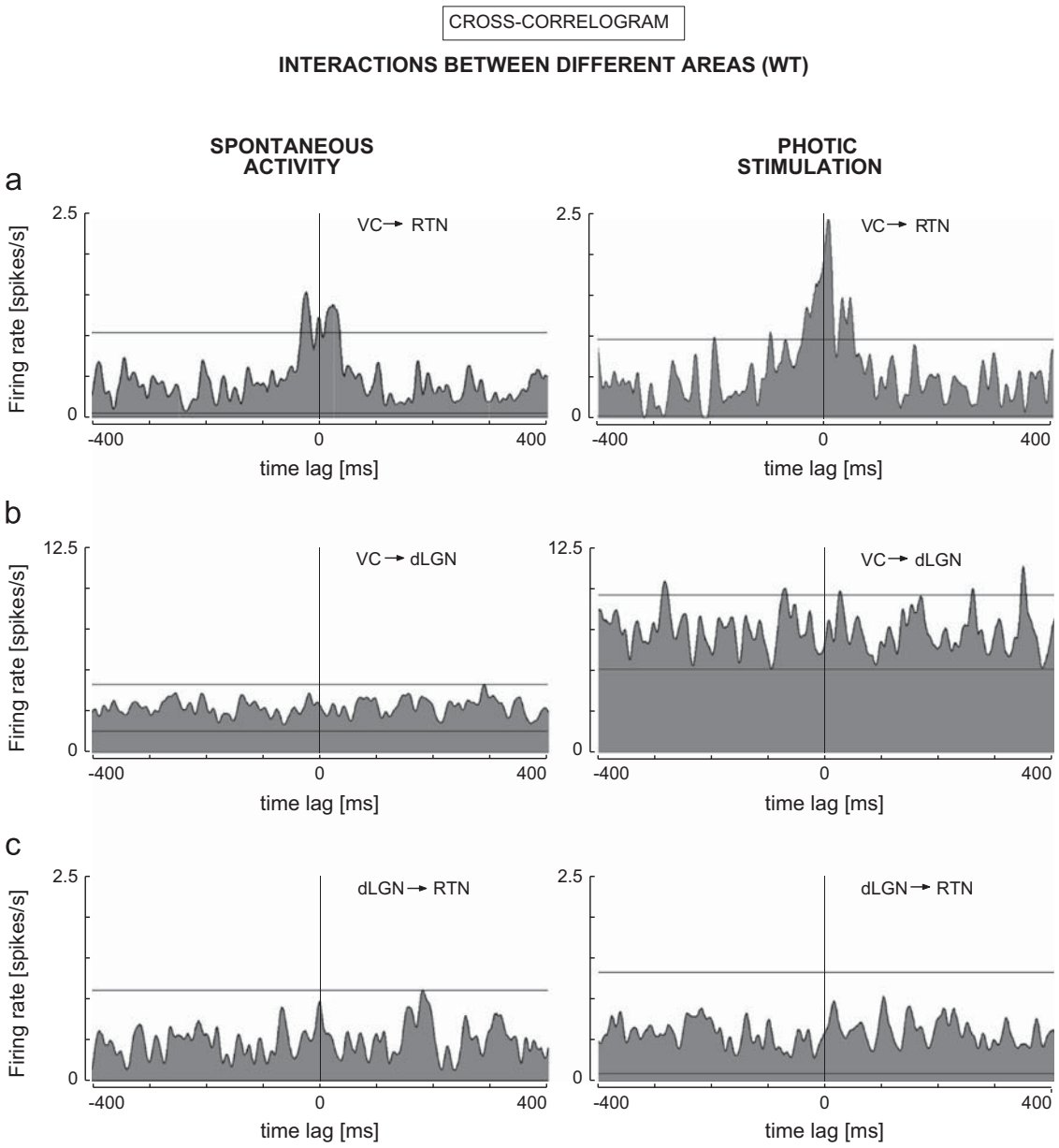

Fig. 5 – Cross-correlograms of selected pairs of units selected from a thalamocortical triplet formed by three cells recorded simultaneously across the three regions of interest of the thalamocortical circuit in a wild-type animal (#TW1). (a) Cell pair with visual cortex (VC) as trigger cell and thalamic reticular nucleus (RTN) as follower cell. (b) Cell pair with VC as trigger cell and dorsal lateral geniculate nucleus (dLGN) as follower cell. (c) Cell pair with dLGN as trigger and RTN as follower cells. The left panels show the cross-correlograms during spontaneous activity and the right panels during the photic stimulation. For axis scaling and labels, refer to Fig. 3.

lesions in the target regions (recordings performed in the left hemisphere). We have mainly recorded from the anterior half of the visual cortex in both groups of animals. No major difference between the sites of recording could be detected after the histological check.

A total of 52 and 71 single units in WT and PVKO, respectively, were characterized by stable firing rate and stable autocorrelogram in the absence of any external stimulation (hereafter referred to as *spontaneous activity*). The analysis of the autocorrelograms during spontaneous activity allows to identify units characterized by a rather flat autocorrelogram ("tonic", firing isolated spikes following Poisson distribution), units that showed a tendency to fire in bursts (bursting) characterized by a large hump in the autocorrelogram near time zero, and units showing a small, lasting less than 40 ms, yet significative deviation from Poisson distribution (irregular). Bursting and tonic modes were observed in RTN, whereas tonic and irregular were mostly observed in VC and dLGN. We did not observe any difference between the distribution of the different firing modes across the regions and across the genotypes, but we must consider that our sample sizes for the firing modes are

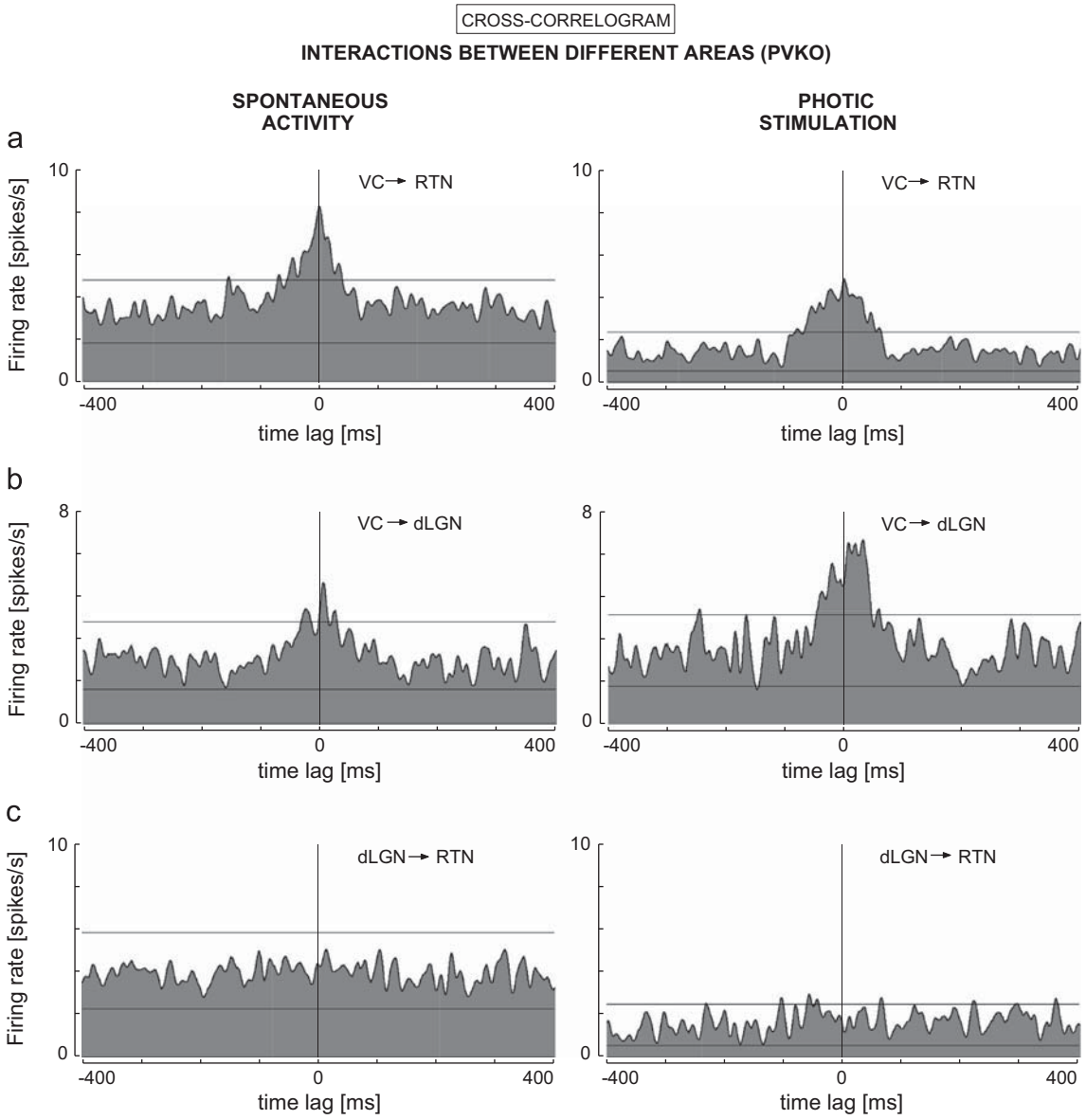

Fig. 6 – Cross-correlograms of selected pairs of units selected from a thalamocortical triplet formed by three cells recorded simultaneously across the three regions of interest of the thalamocortical circuit in a PV-deficient mouse (#TR1). Same legend as Fig. 5.

very limited and do not allow any meaningful statistical comparison. For this reason we decided to pool all cells from each region and analyze the firing rates (Table 1). It is interesting to notice that during spontaneous activity the firing rates tended to be increased in VC and RTN of PVKO mice with respect to WT (Welch *t* test, $t_{(16)} = 3.04$, $2p < 0.01$; $t_{(45)} = 1.82$, $2p < 0.10$, respectively). The same tendency was observed during photic stimulation ($t_{(16)} = 3.90$, $2p < 0.01$; $t_{(44)} = 1.18$, $2p \approx 0.24$, respectively).

We have analyzed the responses to a photic stimulation by a strobe flash at 2.5 Hz. The response patterns were characterized by rapid transients in firing rates with alternations of increases and rebounds in activation followed by suppressions of activity (e.g., two cells in dLGN, Fig. 2). The average firing rates during photic stimulation were not significantly different from the rates observed during spontaneous activity (Table 1). The tendency to an increase in firing during the stimulation was observed in dLGN of either genotypes but was not significant ($t_{(20)} = 1.01$, $2p \approx 0.32$ for WT; $t_{(27)} = 1.27$, $2p \approx 0.26$ for PVKO). The lack of difference between spontaneous and stimulated conditions in the average firing rate is likely to be due to the ripples of activation and inhibition that are evoked by the stroboscopic light. These ripples may be strong and sharp (e.g., Fig. 2a) or blunt and blurred (e.g., Fig. 2b) even for pairs of cells recorded simultaneously from the same electrode tip.

3.2. *Functional interactions between pairs of neighboring cells*

The data of the sample analyzed here include recordings performed at 4 and 5 sites in VC, 7 and 9 sites in RTN, 4 and 6 sites in dLGN of WT and PVKO mice, respectively. At each

site we could record up to 5 cells simultaneously, following the waveform spike sorting procedure. All cell pairs that could be formed between simultaneously recorded cells from the same electrode tip are considered pairs of neighboring cells. Indeed, it is unlikely that the electrode tip can detect a distinguishable bioelectric signal emitted by a neuron that is located at a distance larger than 50–100 μm. Overall we recorded 68 and 94 pairs of neighboring cells in WT and PVKO, respectively.

The functional interactions were classified into three types according to the shape of the cross-correlogram densities calculated according to Abeles (1982b). In case of a curve characterized by a rather symmetrical hump centered near time zero, the cross-correlogram shows a tendency to synchronous firing by the cell pair. The usual interpretation of this shape is that it is assumed that there exists a common synaptic input that contributes to drive the synchronous firing of the cell pair. This type of curve defines the class *common input* (CI). This is a type of functional interaction because it is based on the analysis of the temporal firing pattern, without any anatomical assessment. In case of a flat curve, the cross-correlogram is likely to show *no interaction* (NOI) between the cells. All other shapes of the curve with significant deviations from flatness and without showing a symmetrical hump near time zero are pooled in the class *other*. Table 2 shows the distribution of these three types of functional interactions during spontaneous activity in the regions of interest. In PVKO the CI interactions tended to decrease in all regions (Table 2), but the difference between PVKO and WT was not statistically significant (Fisher's exact test, $2p \approx 0.20$).

Fig. 3a shows the effect of the photic stimulation on a pair of dLGN cells showing a flat curve (no interaction, *NOI*) during spontaneous activity and a trough centered near time zero (*other*) during the stimulation. This trough may suggest a reciprocal inhibition. In case of dLGN, it is likely that the recorded cells are relay cells and that the reciprocal inhibition could be mediated by a RTN GABAergic neuron. The reciprocal inhibition strengthened and triggered by the flash (Fig. 3a) could correspond to an increase of contrast produced via RTN. The synchronization (*CI*) between neighboring cells in RTN (Fig. 3b) was preserved and only slightly decreased by the stimulus presentation. In the visual cortex (VC) the synchronous activity between neighboring cells was usually attuned on a larger time scale, lasting up to 200 ms (e.g., Fig. 4a). In this example the photic stimulation clearly decreased the strength of the synchronization (see how the surface of central hump decreased, Fig. 4a, lower panel) despite an overall increase in firing rate. Another pair of neighboring cells in RTN, recorded in a PVKO, also showed that *CI* tended to decrease during the stimulation (Fig. 4b). Overall we observed that in 19/21 CI in WT and 19/20 CI in PVKO the strobe flash decreased the strength of the functional interaction.

3.3. *Functional interactions across the thalamocortical circuit*

We have analyzed triplets of cells, having one cell in VC, one cell in dLGN and one cell in RTN recorded simultaneously, hereafter referred to as "thalamocortical triplets". Given our sampling, we recorded 294 and 465 thalamocortical triplets in WT and PVKO, respectively. In WT we observed 17 (~6%) triplets with one pair showing significant functional interactions (e.g., Fig. 5), 5 (~6%) triplets with two pairs showing interactions and no triplets with all three significant cross-correlograms. In PVKO we observed 41 (~9%) triplets with one pair showing significant functional interactions, 14 (~6%) triplets with two pairs showing interactions (e.g., Fig. 6) and no triplets with all three significant cross-correlograms. The very limited amount of significant data does not allow a statistical comparison between genotypes. However, irrespective of the genotype, it is interesting to notice that in the majority of the significant cross-correlograms across two different regions of the thalamocortical circuit (e.g., Figs. 5a, 6a, 5b) we observed that the strobe flash tended to increase the interactions, somehow the opposite of what we observed between neighboring cells. Figs. 5a (in WT) and 6a (in PVKO) show examples of a *CI* between VC and RTN that is slightly strengthened during the stimulation. In the case of Fig. 6a it is interesting to notice that the increase in the interaction occurred with an overall firing rate that decreased during the stimulation. In a few cases of *CI* between dLGN and RTN the stimulation provoked the disappearance of the interaction.

4. Discussion

In the present study we have reported for the first time the analysis of in vivo electrophysiological recordings performed simultaneously in the main regions of interest of the visual thalamocortical circuit of the wild-type and parvalbumin-deficient mice. Parvalbumin is a Ca^{2+} buffer protein, which is highly expressed in the vast majority of GABAergic neurons (Celio, 1986, 1990) of the visual thalamocortical circuit and in the retina (Kim and Jeon, 2006). With respect to the visual pathway it is also of interest that PV has been reported to play an important role in the superior colliculus (Lane et al., 1997; Kang et al., 2002). The dynamics of $[Ca^{2+}]_i$ plays a key-role in neuronal cell signaling (Berridge, 1998; Schwaller, 2012a). Hence, a deficiency in PV, which is mainly expressed in inhibitory neurons, is likely to impair the balance between excitation and inhibition in the brain, and particularly along the sensory pathways (Covenas et al., 1991).

It is important to assess our study with one of its major experimental limitations, which is the electrophysiological recording performed under anesthesia. Chloral hydrate alone is not acceptable for anesthesia because it produces mainly a strong sedative effect (Silverman and Muir, 1993; Baxter et al., 2009) and pentobarbital deeply affects the activity of the thalamocortical circuit (Zurita et al., 1994). We used Equithesin, which is a mixture with a lower dose of pentobarbital than that used for a purely pentobarbital induced anesthesia (Deacon and Rawlins, 1996). In rats, in vivo recordings of RTN neurons were performed under pentobarbital, urethane, ketamine, or halothane anesthesia aiming primarily to study the comparative response to nociceptive stimuli in RTN and in the ventroposterior lateral nucleus of the thalamus (Yen and Shaw, 2003). Various general anesthetics were compared in rats (Field et al., 1993) and mice (Erhardt et al., 1984). The combination of ketamine and xylazine might be considered the most reliable for anesthesia of mice, despite that respiration was moderately decreased and the cardiovascular

system was strongly depressed. However, ketamine/xylazine anesthesia in mice showed different regional effects in the thalamus (Kim et al., 2012), i.e. that the ventral lateral thalamus Granger-caused the primary motor cortex and the primary somatosensory cortex, whereas the primary somatosensory cortex consistently Granger-caused the ventrobasal thalamus, regardless of the loss of consciousness. In the visual thalamocortical pathway tuning properties in the awake animals were similar to those measured previously in anesthetized animals (Niell and Stryker, 2010). These authors showed that visually evoked firing rates in VC were reported to increase significantly during running, but in the lateral geniculate nucleus did not increase with locomotion.

The response gain of neurons in the visual cortex is under the control of GABA(A) mediated inhibition (Liu et al., 2010; Katzner et al., 2011), associated to PV-containing interneurons (Atallah et al., 2012; Runyan et al., 2010). We have observed that the lack of PV does indeed significantly increase the firing rate of neurons of the visual cortex in the absence as well as in the presence of a visual stimulation. We found that cells in RTN tended to fire at a higher rate in PVKO, in agreement with Albéri et al. (in press). This is the first study, to our knowledge, to report data on the firing pattern of dLGN cells in PV-deficient mice. Interestingly, dLGN cells in PVKO did not show significant changes in the rate of firing. The study of the response patterns to visual stimuli was beyond our aim and we limited our study to a photic stimulus with a strobe flash. We observed transient responses to the flashes with latencies and patterns comparable to other studies reported in the literature for the dLGN (Grubb and Thompson, 2005) and visual cortex (Mangini and Pearlman, 1980; Métin et al., 1988; Niell and Stryker, 2010). The role of PV in the retina and superior colliculus suggests that the afferent visual information to the thalamocortical circuit is likely to be altered in the PVKO and we will not discuss further visual processing features.

We have analyzed the pattern of functional interactions between pairs of neighboring cells in VC, dLGN and RTN and across these areas in simultaneously recorded thalamocortical triplets, with one cell from each area. The main finding here is that in PVKO the strength of the interactions tended to decrease locally, between neighboring cells, but tended to increase across the areas. The only comparison of these results that is possible with other data is the decrease of common inputs in RTN of PVKO reported elsewhere in a different series of experiments under different anesthetic conditions (Albéri et al., in press). Our overall finding suggests that the ability to process information along parallel channels is decreased in the thalamocortical pathway of PV-deficient mice. Less local interaction would correspond to less local coherency in information processing, which is in agreement with a widespread processing that would involve larger areas, thus leading to increased correlation across regions. It is worth to notice an increase in the variance of the firing rate of VC and RTN neurons of PVKO with respect to WT (Table 1) and, on the opposite, a decrease in the firing rate variance of dLGN. These observations might suggest that the perturbation produced by the lack of PV may let appear a heterogeneity in the cell properties of VC and RTN neurons at rest that was not possible to notice in WT. This effect would be similar what was observed at the level of the firing properties of thalamic neurons during cortical cooling (Villa et al., 1991). Nevertheless, we are aware that our samples are very limited in size and we cannot discard a bias in our results due to the sampling and to the fact that we have recorded from the anterior half of the visual cortex.

An essential aspect to consider in the interpretation of results obtained in transgenic mouse models is whether the effects are caused by the deletion/mutation of the gene product of interest (in our study PV) or possibly due to a homeostatic remodeling induced by the genetic manipulation(s). A way to testing for these two possibilities consists of reconstituting the deleted protein or the addition of a component expected to substitute for the missing protein. In the best circumstance this leads to restoring of the WT phenotype. In the case of the slow-onset calcium buffer PV, the most closely related exogenous substitute is the slow calcium chelator EGTA. Addition of 1 mM EGTA to PVKO molecular layer interneurons (MLI) restores paired-pulse depression between MLI and Purkinje cells, while otherwise in PVKO paired-pulse facilitation predominates at this synapse (Caillard et al., 2000). Similarly in presynaptic PV-expressing terminals in the calyx of Held, the shape of AP-induced increase in $[Ca^{2+}]_i$ and associated facilitation could be rescued in PVKO mice by either applying PV or EGTA (0.1 mM) (Müller et al., 2007). Also, in striatal fast-spiking interneurons of PVKO mice, the increased excitability is reverted close to the WT situation by adding EGTA to the patch pipette (Orduz et al., in press). Furthermore, PV expression in the mouse brain starts relatively late commencing between postnatal day 10 (P10) and P14 as evidenced in the neocortex (del Río et al., 1994) and in the cerebellum (Collin et al., 2005); not surprisingly, no principal differences in the distribution and morphology of "PV-ir" neurons in PVKO mice are observed, neither in the hippocampus (Vreugdenhil et al., 2003) nor the cortex (Schwaller et al., 2004). All these results strongly support our hypothesis that changes observed in PVKO mice are mostly the direct result of PV's absence, rather than caused by compensation mechanisms in these mice. It is rationale to assume that a similar situation also pertains to the population of PV-ir neurons in the RTN, dLGN and VC. However, we are aware that we have not directly addressed the question in these neuron subpopulations.

A decrease in the expression of PV is associated with epileptic seizure susceptibility (Marco et al., 1997; Schwaller et al., 2004), mild behavioral and motor alterations (Farré-Castany et al., 2007), schizophrenia (Pinault, 2011; Lewis et al., 2012), bipolar disorder (Berridge, 2013) and autism spectrum disorder (Oblak et al., 2011). In particular, a reduction in the density of parvalbumin-positive neurons, and schizophrenic traits have recently been demonstrated in the methyl azoxymethanol acetate model of schizophrenia (Lodge et al., 2009). The impaired balance between excitatory and inhibitory in sensory system was proposed as model for the autism (Rubenstein and Rakic, 1999). This vast body of evidence suggests that PV-deficiency provokes a severe alteration in neuromodulatory transmission of sensory information processing that affects perception and might affect attentional and cognitive mechanisms in the thalamocortical circuit (Pinault, 2011; Kulikova et al., 2012). These results emphasize that the sensory thalamic nuclei, dLGN for the visual pathway, cannot be merely considered as relay nuclei, but should

be considered as part of a network, the thalamocortical circuit that plays a key-role in filtering the sensory afferent information that is fed to the cerebral cortex, according to the "adaptive filtering hypothesis" (Villa and Tetko, 1997). Hence, PV-expression would control such filtering with the consequence to produce a fan-effect in the perceptive thoughts in case of PV deficiency, which is part of the symptoms reported by the patients affected by the neuropsychiatric disorders mentioned above. In the thalamocortical circuit, RTN, which is almost exclusively formed by PV-ir cells, occupies a particularly important place to modulate the intrageniculate excitatory/inhibitory balance as suggested by corticofugal studies (Villa et al., 1999; Alexander et al., 2006; Augustinaite et al., 2011). In conclusion, thanks to the combined study of the firing pattern, local functional interaction and functional interactions across the thalamocortical circuit, the current study provides new evidence on the important role played by PV in regulating information processing in the central visual pathway.

Acknowledgments

We acknowledge the support received by the Swiss National Science Foundation SNSF Grant # 130680 and by Prof. Robert Kretz. We wish to thank M. Kaczorowski and F. Filice for their technical assistance with the histological procedures.

REFERENCES

Abeles, M., 1982a. Local Cortical Circuits. Springer Verlag.
Abeles, M., 1982b. Quantification, smoothing, and confidence limits for single-units' histograms. J. Neurosci. Methods 5, 317–325.
Aksenova, T.I., Chibirova, O.K., Dryga, O.A., Tetko, I.V., Benabid, A. L., Villa, A.E.P., 2003. An unsupervised automatic method for sorting neuronal spike waveforms in awake and freely moving animals. Methods 30, 178–187.
Albéri, L., Lintas, A., Kretz, R., Schwaller, B., Villa, A.E.P., 2013. The calcium-binding protein parvalbumin modulates the firing properties of the reticular thalamic nucleus bursting neurons. J. Neurophysiol, http://dx.doi.org/10.1152/jn.00375.2012, in press.
Alexander, G.M., Fisher, T.L., Godwin, D.W., 2006. Differential response dynamics of corticothalamic glutamatergic synapses in the lateral geniculate nucleus and thalamic reticular nucleus. Neuroscience 137, 367–372.
Arcelli, P., Frassoni, C., Regondi, M.C., De Biasi, S., Spreafico, R., 1997. Gabaergic neurons in mammalian thalamus: a marker of thalamic complexity? Brain Res. Bull. 42, 27–37.
Asai, Y., Aksenova, T.I., Villa, A.E.P., 2005. Unsupervised Recognition of Neuronal Discharge Waveforms for On-line Real-time Operation. Lecture Notes in Computer Science, vol. 3704, pp. 29–38.
Atallah, B.V., Bruns, W., Carandini, M., Scanziani, M., 2012. Parvalbumin-expressing interneurons linearly transform cortical responses to visual stimuli. Neuron 73, 159–170.
Augustinaite, S., Yanagawa, Y., Heggelund, P., 2011. Cortical feedback regulation of input to visual cortex: role of intrageniculate interneurons. J. Physiol. 589, 2963–2977.
Baldauf, Z.B., 2010. Dual chemoarchitectonic lamination of the visual sector of the thalamic reticular nucleus. Neuroscience 165, 801–818.
Baxter, M.G., Murphy, K.L., Taylor, P.M., Wolfensohn, S.E., 2009. Chloral hydrate is not acceptable for anesthesia or euthanasia of small animals. Anesthesiology 111, 209–210.
Berridge, M.J., 1998. Neuronal calcium signaling. Neuron 21, 13–26.
Berridge, M.J., 2013. Dysregulation of neural calcium signaling in Alzheimer disease, bipolar disorder and schizophrenia. Prion 6, 2–13.
Bickford, M.E., Slusarczyk, A., Dilger, E.K., Krahe, T.E., Kucuk, C., Guido, W., 2010. Synaptic development of the mouse dorsal lateral geniculate nucleus. J. Comp. Neurol. 518, 622–635.
Caillard, O., Moreno, H., Schwaller, B., Llano, I., Celio, M.R., Marty, A., 2000. Role of the calcium-binding protein parvalbumin in short-term synaptic plasticity. Proc. Natl. Acad. Sci. USA 97, 13372–13377.
Cardin, J.A., Carlén, M., Meletis, K., Knoblich, U., Zhang, F., Deisseroth, K., Tsai, L.H., Moore, C.I., 2009. Driving fast-spiking cells induces gamma rhythm and controls sensory responses. Nature 459, 663–667.
Celio, M.R., 1986. Parvalbumin in most gamma-aminobutyric acid-containing neurons of the rat cerebral cortex. Science 231, 995–997.
Celio, M.R., 1990. Calbindin D-28k and parvalbumin in the rat nervous system. Neuroscience 35, 375–475.
Chattopadhyaya, B., Di Cristo, G., Wu, C.Z., Knott, G., Kuhlman, S., Fu, Y., Palmiter, R.D., Huang, Z.J., 2007. Gad67-mediated gaba synthesis and signaling regulate inhibitory synaptic innervation in the visual cortex. Neuron 54, 889–903.
Coleman, J.E., Law, K., Bear, M.F., 2009. Anatomical origins of ocular dominance in mouse primary visual cortex. Neuroscience 161, 561–571.
Collin, T., Chat, M., Lucas, M.G., Moreno, H., Racay, P., Schwaller, B., Marty, A., Llano, I., 2005. Developmental changes in parvalbumin regulate presynaptic Ca2+ signaling. J. Neurosci. 25, 96–107.
Coveñas, R., De León, M., Alonso, J.R., Arévalo, R., Lara, J., Aijón, J., 1991. Distribution of parvalbumin-immunoreactivity in the rat thalamus using a monoclonal antibody. Arch. Ital. Biol. 129, 199–210.
Deacon, R.M., Rawlins, J.N., 1996. Equithesin without chloral hydrate as an anaesthetic for rats. Psychopharmacology (Berl.) 124, 288–290.
Dräger, U.C., 1975. Receptive fields of single cells and topography in mouse visual cortex. J. Comp. Neurol. 160, 269–290.
Dräger, U.C., Olsen, J.F., 1980. Origins of crossed and uncrossed retinal projections in pigmented and albino mice. J. Comp. Neurol. 191, 383–412.
Endo, T., Kobayashi, M., Kobayashi, S., Onaya, T., 1986. Immunocytochemical and biochemical localization of parvalbumin in the retina. Cell Tissue Res. 243, 213–217.
Erhardt, W., Hebestedt, A., Aschenbrenner, G., Pichotka, B., Blümel, G., 1984. A comparative study with various anesthetics in mice (pentobarbitone, ketamine-xylazine, carfentanyl–etomidate). Res. Exp. Med. (Berl.) 184, 159–169.
Farré-Castany, M.A., Schwaller, B., Gregory, P., Barski, J., Mariethoz, C., Eriksson, J.L., Tetko, I.V., Wolfer, D., Celio, M.R., Schmutz, I., Albrecht, U., Villa, A.E., 2007. Differences in locomotor behavior revealed in mice deficient for the calcium-binding proteins parvalbumin, calbindin d-28k or both. Behav. Brain Res. 178, 250–261.
Field, K.J., White, W.J., Lang, C.M., 1993. Anaesthetic effects of chloral hydrate, pentobarbitone and urethane in adult male rats. Lab. Anim. 27, 258–269.
Gonchar, Y., Wang, Q., Burkhalter, A., 2008. Multiple distinct subtypes of GABAergic neurons in mouse visual cortex identified by triple immunostaining. Front. Neuroanat. 1, e003.
Grubb, M.S., Thompson, I.D., 2005. Visual response properties of burst and tonic firing in the mouse dorsal lateral geniculate nucleus. J. Neurophysiol. 93, 3224–3247.

Heizmann, C.W., Braun, K., 1992. Changes in Ca(2+)-binding proteins in human neurodegenerative disorders. Trends Neurosci. 15, 259–264.
Hübener, M., 2003. Mouse visual cortex. Curr. Opin. Neurobiol. 13, 413–420.
Jaubert-Miazza, L., Green, E., Lo, F.S., Bui, K., Mills, J., Guido, W., 2005. Structural and functional composition of the developing retinogeniculate pathway in the mouse. Vis. Neurosci. 22, 661–676.
Jones, E.G., Hendry, S.H., 1989. Differential calcium binding protein immunoreactivity distinguishes classes of relay neurons in monkey thalamic nuclei. Eur. J. Neurosci. 1, 222–246.
Jurgens, C.W., Bell, K.A., McQuiston, A.R., Guido, W., 2012. Optogenetic stimulation of the corticothalamic pathway affects relay cells and gabaergic neurons differently in the mouse visual thalamus. PLoS One 7, e0045717.
Kang, Y.S., Park, W.M., Lim, J.K., Kim, S.Y., Jeon, C.J., 2002. Changes of calretinin, calbindin D28K and parvalbumin-immunoreactive neurons in the superficial layers of the hamster superior colliculus following monocular enucleation. Neurosci. Lett. 330, 104–108.
Katzner, S., Busse, L., Carandini, M., 2011. GABA(A) inhibition controls response gain in visual cortex. J. Neurosci. 31, 5931–5941.
Kim, S.P., Hwang, E., Kang, J.H., Kim, S., Choi, J.H., 2012. Changes in the thalamocortical connectivity during anesthesia-induced transitions in consciousness. Neuroreport 23, 294–298.
Kim, T.J., Jeon, C.J., 2006. Morphological classification of parvalbumin-containing retinal ganglion cells in mouse: single-cell injection after immunocytochemistry. Invest. Ophthalmol. Vis. Sci. 47, 2757–2764.
Krahe, T.E., El-Danaf, R.N., Dilger, E.K., Henderson, S.C., Guido, W., 2011. Morphologically distinct classes of relay cells exhibit regional preferences in the dorsal lateral geniculate nucleus of the mouse. J. Neurosci. 31, 17437–17448.
Kulikova, S.P., Tolmacheva, E.A., Anderson, P., Gaudias, J., Adams, B.E., Zheng, T., Pinault, D., 2012. Opposite effects of ketamine and deep brain stimulation on rat thalamocortical information processing. Eur. J. Neurosci. 36, 3407–3419.
Lane, R.D., Allan, D.M., Bennett-Clarke, C.A., Howell, D.L., Rhoades, R. W., 1997. Projection status of calbindin- and parvalbumin-immunoreactive neurons in the superficial layers of the rat's superior colliculus. Vis. Neurosci. 14, 277–286.
Lee, S.H., Schwaller, B., Neher, E., 2000. Kinetics of Ca2+ binding to parvalbumin in bovine chromaffin cells: implications for [Ca2+] transients of neuronal dendrites. J. Physiol. 525, 419–432.
Lewis, D.A., Curley, A.A., Glausier, J.R., Volk, D.W., 2012. Cortical parvalbumin interneurons and cognitive dysfunction in schizophrenia. Trends Neurosci. 35, 57–67.
Linden, M.L., Heynen, A.J., Haslinger, R.H., Bear, M.F., 2009. Thalamic activity that drives visual cortical plasticity. Nat. Neurosci. 12, 390–392.
Lintas, A., Silkis, I.G., Albéri, L., Villa, A.E., 2012. Dopamine deficiency increases synchronized activity in the rat subthalamic nucleus. Brain Res. 1434, 142–151.
Liu, B.H., Li, P., Sun, Y.J., Li, Y.T., Zhang, L.I., Tao, H.W., 2010. Intervening inhibition underlies simple-cell receptive field structure in visual cortex. Nat. Neurosci. 13, 89–96.
Lodge, D.J., Behrens, M.M., Grace, A.A., 2009. A loss of parvalbumin-containing interneurons is associated with diminished oscillatory activity in an animal model of schizophrenia. J. Neurosci. 29, 2344–2354.
Mangini, N.J., Pearlman, A.L., 1980. Laminar distribution of receptive field properties in the primary visual cortex of the mouse. J. Comp. Neurol. 193, 203–222.
Marco, P., Sola, R.G., Ramón y Cajal, S., DeFelipe, J., 1997. Loss of inhibitory synapses on the soma and axon initial segment of pyramidal cells in human epileptic peritumoural neocortex: implications for epilepsy. Brain Res. Bull. 44, 47–66.
Métin, C., Godement, P., Imbert, M., 1988. The primary visual cortex in the mouse: receptive field properties and functional organization. Exp. Brain Res. 69, 594–612.
Moreno, H., Burghardt, N.S., Vela-Duarte, D., Masciotti, J., Hua, F., Fenton, A.A., Schwaller, B., Small, S.A., 2011. The absence of the calcium-buffering protein calbindin is associated with faster age-related decline in hippocampal metabolism. Hippocampus 22, 1107–1120.
Müller, M., Felmy, F., Schwaller, B., Schneggenburger, R., 2007. Parvalbumin is a mobile presynaptic Ca2+ buffer in the calyx of held that accelerates the decay of Ca2+ and short-term facilitation. J. Neurosci. 27, 2261–2271.
Niell, C.M., Stryker, M.P., 2010. Modulation of visual responses by behavioral state in mouse visual cortex. Neuron 65, 472–479.
Oblak, A.L., Rosene, D.L., Kemper, T.L., Bauman, M.L., Blatt, G.J., 2011. Altered posterior cingulate cortical cyctoarchitecture, but normal density of neurons and interneurons in the posterior cingulate cortex and fusiform gyrus in autism. Autism Res. 4, 200–211.
Orduz, D., Bischop, P., Schwaller, B., Schiffmann, S.N., Gall, D. Parvalbumin tunes spike-timing and efferent short-term plasticity in striatal fast spiking interneurons. J. Physiol., http://dx.doi.org/10.1113/jphysiol.2012.250795., in press.
Parajuli, L.K., Fukazawa, Y., Watanabe, M., Shigemoto, R., 2010. Subcellular distribution of α1G subunit of T-type calcium channel in the mouse dorsal lateral geniculate nucleus. J. Comp. Neurol. 518, 4362–4374.
Paxinos, G., Franklin, K., 2001. The Mouse Brain in Stereotaxic Coordinates, 2nd edition Academic Press, New York.
Petrof, I., Viaene, A.N., Sherman, S.M., 2012. Two populations of corticothalamic and interareal corticocortical cells in the subgranular layers of the mouse primary sensory cortices. J. Comp. Neurol. 520, 1678–1686.
Pinault, D., 2011. Dysfunctional thalamus-related networks in schizophrenia. Schizophr. Bull. 37, 238–243.
Prusky, G.T., West, P.W., Douglas, R.M., 2000. Behavioral assessment of visual acuity in mice and rats. Vision Res. 40, 2201–2209.
Rafols, J.A., Valverde, F., 1973. The structure of the dorsal lateral geniculate nucleus in the mouse. A Golgi and electron microscopic study. J. Comp. Neurol. 150, 303–332.
del Río, J.A., de Lecea, L., Ferrer, I., Soriano, E., 1994. The development of parvalbumin-immunoreactivity in the neocortex of the mouse. Brain Res. Dev. Brain Res. 81, 247–259.
Rubenstein, J.L., Rakic, P., 1999. Genetic control of cortical development. Cerebral Cortex 9, 521–523.
Runyan, C.A., Schummers, J., Van Wart, A., Kuhlman, S.J., Wilson, N.R., Huang, Z.J., Sur, M., 2010. Response features of parvalbumin-expressing interneurons suggest precise roles for subtypes of inhibition in visual cortex. Neuron 67, 847–857.
Sanna, P.P., Keyser, K.T., Celio, M.R., Karten, H.J., Bloom, F.E., 1993. Distribution of parvalbumin immunoreactivity in the vertebrate retina. Brain Res. 600, 141–150.
Schwaller, B., 2010. Cytosolic Ca2+ buffers. Cold Spring Harb. Perspect. Biol. 2, a004051.
Schwaller, B., 2012a. The regulation of a cell's Ca2+ signaling toolkit: the Ca2+ homeostasome. Adv. Exp. Med. Biol. 740, 1–25.
Schwaller, B., 2012b. The use of transgenic mouse models to reveal the functions of Ca2+ buffer proteins in excitable cells. Biochim. Biophys. Acta 1820, 1294–1303.
Schwaller, B., Dick, J., Dhoot, G., Carroll, S., Vrbova, G., Nicotera, P., Pette, D., Wyss, A., Bluethmann, H., Hunziker, W., Celio, M. R., 1999. Prolonged contraction–relaxation cycle of fast-twitch muscles in parvalbumin knockout mice. Am. J. Physiol. 276, 395–403.

Schwaller, B., Tetko, I.V., Tandon, P., Silveira, D.C., Vreugdenhil, M., Henzi, T., Potier, M.C., Celio, M.R., Villa, A.E., 2004. Parvalbumin deficiency affects network properties resulting in increased susceptibility to epileptic seizures. Mol. Cell. Neurosci. 25, 650–663.
Sherman, S.M., Guillery, R.W., 2011. Distinct functions for direct and transthalamic corticocortical connections. J. Neurophysiol. 106, 1068–1077.
Silverman, J., Muir, W.W., 1993. A review of laboratory animal anesthesia with chloral hydrate and chloralose. Lab. Anim. Sci. 43, 210–216.
Smith, S.L., Häusser, M., 2010. Parallel processing of visual space by neighboring neurons in mouse visual cortex. Nat. Neurosci. 13, 1144–1149.
Tanahira, C., Higo, S., Watanabe, K., Tomioka, R., Ebihara, S., Kaneko, T., Tamamaki, N., 2009. Parvalbumin neurons in the forebrain as revealed by parvalbumin-Cre transgenic mice. Neurosci. Res. 63, 213–223.
Villa, A.E.P., Rouiller, E.M., Simm, G., Zurita, P., de Ribaupierre, Y., de Ribaupierre, F., 1991. Corticofugal modulation of the information processing in the auditory thalamus of the cat. Exp. Brain Res. 86, 506–517.
Villa, A.E.P., Tetko, I.V., 1997. Efficient partition of learning data sets for neural network training. Neural Networks 10, 1361–1374.
Villa, A.E.P., Tetko, I.V., Dutoit, P., de Ribaupierre, Y., de Ribaupierre, F., 1999. Corticofugal modulation of functional connectivity within the auditory thalamus of rat, guinea pig and cat revealed by cooling deactivation. J. Neurosci. Methods 86, 161–178.
Vreugdenhil, M., Jefferys, J.G., Celio, M.R., Schwaller, B., 2003. Parvalbumin-deficiency facilitates repetitive IPSCs and gamma oscillations in the hippocampus. J. Neurophysiol. 89, 1414–1422.
Yen, C.T., Shaw, F.Z., 2003. Reticular thalamic responses to nociceptive inputs in anesthetized rats. Brain Res. 968, 179–191.
Zhan, X.J., Cox, C.L., Sherman, S.M., 2000. Dendritic depolarization efficiently attenuates low-threshold calcium spikes in thalamic relay cells. J. Neurosci. 20, 3909–3914.
Zurita, P., Villa, A.E.P., de Ribaupierre, Y., De Ribaupierre, F., Rouiller, E., 1994. Changes of single unit activity in the cat's auditory thalamus and cortex associated to different anesthetic conditions. Neurosci. Res. 19, 303–316.